The brown-black continuum of light-absorbing combustion aerosols

Rawad Saleh*, Zezhen Cheng, Khairallah Atwi

Air Quality and Climate Research Laboratory, University of Georgia, 110 Riverbend Road, Athens, GA 30602, USA

School of Environmental, Civil, Agricultural, and Mechanical Engineering, University of Georgia, 597 D.W. Brooks Drive, Athens, GA 30602, USA

^{*}To whom correspondence should be addressed. rawad@uga.edu, (706) 542-6110

Abstract

Brown carbon (BrC) exhibits highly variable light-absorption properties with imaginary part of the refractive indices (k) varying over several orders of magnitude. This poorly understood variability poses a challenge to accurately determining the BrC climate effect. Here, we present a framework to explain the variability in BrC k. We hypothesize that a fraction of BrC is comprised of black-carbon (BC) precursors whose transformation to BC is not complete and that there is a continuum of light-absorption properties along which BC and BrC lie. To test this hypothesis, we performed controlled-combustion experiments using benzene and toluene. By systematically varying the combustion conditions, we isolated BrC components along the brown-black continuum progressing from light (k = 0.004 at 550 nm) to dark (k = 0.25 at 550 nm). Using laser-desorption-ionization mass spectrometry and thermodenuder measurements, we show that the BrC progression from light to dark is associated with increase in molecular size and decrease in volatility. The darkest BrC has molecular sizes of several 1000 Da, is refractory, and is optically more similar to BC than the lighter BrC, blurring the lines between the optical properties of BrC and BC.

Keywords: brown carbon, aerosol, combustion, light absorption, climate

Introduction

Brown carbon (BrC), the light-absorbing fraction of organic aerosol, is an important yet poorly characterized climate warmer. It is often co-emitted with black carbon (BC) by incomplete combustion of biomass fuels and can also form through secondary reactions in the atmosphere. In this paper, we focus on combustion BrC.

It is informative to contrast the state of science of BrC with that of BC. While the role of BC as a leading climate warmer was discovered at the turn of the century, 16,17 its climate effect is still highly uncertain. Consisting mostly of elemental carbon, BC is defined as the refractory, fractal, highly absorptive fraction of carbonaceous aerosols. The light-absorption properties of BC are characterized by a well-constrained wavelength-independent imaginary part of the refractive index (k). The uncertainty in the BC climate effect is largely due to challenges on the climate-calculation level, including the inability to accurately represent the BC burden, lifetime, and mixing state and morphology. BrC, on the other hand, is poorly understood on the fundamental level. There are major gaps in our knowledge of its formation pathways and optical properties. The BrC k values reported in the literature span several orders of magnitude. A4,6,26,27 While there have been a number of recent attempts to include the BrC effect in climate calculations, $^{21,23,28-30}$ this endeavor is in its infancy and still requires substantial iterations with fundamental and experimental investigations.

BrC-producing combustion is chaotic. Therefore, it seems imperative that BrC characterization should rely on measurements that feature similar conditions in order to obtain atmospherically relevant results. BrC investigations have strived to achieve such conditions by performing atmospheric measurements^{9,10,26,27,31–33} or laboratory experiments that simulated real-life uncontrolled combustion.^{3,4,6–8,34} While atmospheric relevancy is certainly a merit, there is a crucial drawback: the inherent variability in combustion has led to the aforementioned large variability in

reported BrC *k* and has made it challenging to identify the source of this variability. This calls for a fundamental investigation of BrC, which we are set to achieve in this paper.

Brown carbon formation in combustion

BrC exhibits highly diverse chemical structures.²⁵ Among the most frequently detected atmospheric BrC components are nitroaromatic compounds, including nitrophenols and nitrocatechols.^{34–37,10} These compounds are expected to form via secondary reactions in the atmosphere^{35,36,10} and are unlikely to account for BrC produced during combustion. BrC components linked to biomass combustion include charge transfer complexes³⁸ and tar balls.³⁹ A comprehensive understanding of the most important combustion BrC components, however, is still lacking.²⁵

We hypothesize that an important fraction of combustion BrC is comprised of organic precursors of BC whose transformation to BC is not complete during the combustion process. Depending on the combustion conditions, these BC precursors exhibit different maturity levels which dictate their light-absorption properties. The more mature the precursors are, the more absorptive (BC-like) they become. Therefore, the light-absorption properties of BrC obtained from a certain measurement depend on the specific combustion conditions associated with the measurement. We have previously observed this behavior in biomass-combustion emissions, where combustion conditions that were more conducive to BC formation produced darker BrC. BC, on the other hand, is the end product to which the precursors converge, leading to the uniformity in BC molecular structure and optical properties.

This hypothesis finds support in the combustion literature. In a combustion process, the initial steps towards BC inception are marked by the formation of small polycyclic aromatic hydrocarbons (PAHs). As the temperature increases, these PAHs undergo growth by collisions to form large oligomeric structures. 40-42 Stein and Fahr 43 performed thermodynamic calculations showing that only a certain class of PAHs can survive fragmentation at each stage of the combustion reaction and that their molecular sizes increase as the combustion progresses towards BC inception. When the PAHs reach large molecular sizes that can no longer maintain planar structures, they warp into 3-D structures, marking the onset of carbonization, or BC inception. 44 These PAHs exhibit significant UV-vis absorption spectra. 41,44-47 In other words, they are BrC.

The brown-black continuum hypothesis can be tested by performing combustion experiments with well-constrained conditions. By varying the combustion conditions to progressively approach the BC-formation threshold, the different BrC components along the continuum can be isolated and their k can be retrieved. Progression towards the BC-inception threshold is accompanied by increase in molecular size,⁴⁸ and since volatility is dependent on molecular size,⁴⁹ the increase in molecular size is expected to be accompanied by decrease in volatility. Therefore, the brown-black continuum hypothesis predicts association between BrC darkness, molecular size, and volatility.

Materials and methods

Since in any combustion process the first critical step towards BC inception is the formation of aromatic rings,⁴⁸ we chose benzene and toluene as model fuels. We performed combustion experiments controlled at temperatures ranging between 750 °C and 1050 °C and equivalence ratios (actual fuel-to-air ratio divided by the stoichiometric fuel-to-air ratio) between 1 and 1.7. Combustion took place in a custom-made quartz chamber enclosed in a temperature-controlled heater. Fuel was introduced into the combustion chamber by flowing air through a bubbler containing the fuel, thus saturating the air with fuel. We mixed additional clean air with the fuel-saturated air to adjust the equivalence ratio and used pure nitrogen as a passive diluent^{50,51} to fine-tune the combustion conditions. The combustion conditions for all experiments are listed in Table S1.

We performed optical closure^{4,6,7,9} to retrieve k of BrC produced at different combustion conditions. Optical closure involved fitting Mie theory calculations to absorption coefficients measured in real-time using a 3-wavelength (422, 532, and 785 nm) photoacoustic spectrophotometer.⁵² We represent the wavelength-dependent k as $k = k_{550}$ [$550/\lambda$]^w, where k_{550} is imaginary part of the refractive index at a wavelength (λ) of 550 nm and w is the wavelength dependence. For readers more familiar with the absorption Ångström exponent (AAE) as a measure of the wavelength dependence of aerosol light absorption, AAE = w + 1 for particles much smaller than λ . However, AAE depends on particle size and thus the equality does not hold for particle sizes approaching λ . For some experiments, we heated the BrC in a thermodenuder at 100 °C, 200 °C, 300 °C, and 400 °C and retrieved k of the BrC fraction that did not evaporate. The thermodenuder measurements also served as a means to compare the volatilities of the BrC produced at different combustion conditions.

To investigate the association between BrC darkness and molecular size, we employed laser desorption ionization mass spectrometry (LDI-MS).^{40,45,53} The advantage of LDI is that it is softionizing and thus allows the detection of the large PAHs that we hypothesize to constitute BrC with minimal fragmentation. However, quantitative measurements with LDI-MS are challenging due to laser-induced reactions that could lead to clustering, as well as differences in desorption and ionization efficiencies between different molecules.⁵⁴ A frequently observed artifact is the reduction in signal intensity with increasing molecular size.⁵⁴ Since artifacts associated with LDI depend on operating conditions,⁵⁵ one can make qualitative comparisons between mass spectra of samples obtained under the same LDI operating conditions.

Results and Discussion

Figure 1a shows k_{550} versus w retrieved from the controlled-combustion experiments. Starting with the simple benzene and toluene molecules, we produced a myriad of BrC components with stark diversity in their light-absorption properties. The k_{550} and w range from 0.004 and 8.6 to 0.25 and 0.5. These ranges are similar to those reported in the literature for biomass-combustion BrC. 3,47,26,27,56,57 Furthermore, k_{550} and w are well-correlated and exhibit an exponential-decay functional dependence. Each k_{550} -w pair in Figure 1a represents an "optical bin" along the brownblack continuum. As the combustion conditions approach the BC-formation threshold (increase in temperature and/or decrease in equivalence ratio), k_{550} increases and w decreases, indicating

that BrC becomes darker (its optical properties are closer to BC). This is visually illustrated by the three filter samples shown in Figure 1b, representative of relatively light (**A**), medium (**B**), and dark (**C**) BrC. Real-life uncontrolled combustion produces a range of BrC components that can be represented as probability distributions along the optical bins represented in Figure 1. BC has $k_{550} \approx 0.6$ -0.8 and $w \approx 0,^{20}$ which, as shown in Figure 1c, falls on the exponential-decay function fitting the BrC k_{550} and w. This suggests that the different BrC components and BC lie on the same continuum of light-absorption properties.

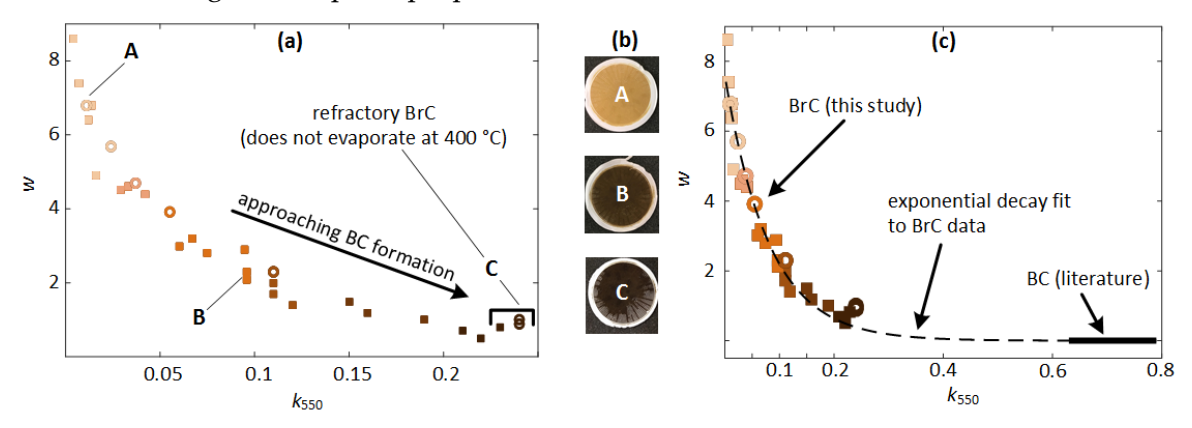


Figure 1 The continuum of light-absorption properties of BrC emitted by benzene (solid squares) and toluene (open circles) combustion controlled at different temperatures (750 °C – 1050 °C) and equivalence ratios (1 – 1.7). (a) The wavelength dependence of the imaginary part of the refractive index (w) versus the imaginary part of the refractive index at 550 nm (k550). Each data point represents a 30-minute average (see SI for details). The color gradient of the data points signifies progressively darker BrC as the combustion conditions approach BC formation. Some of the data points correspond to thermodenuder measurements, where the BrC was heated to temperatures between 100 °C and 400 °C, and k550 and w of the residual BrC were retrieved. Of special interest are the data points obtained at 400 °C, which constitute refractory BrC (rBrC), the darkest BrC that we isolated in this study. The calculated standard deviations of k550 and w are smaller than the size of the symbols. (b) Pictures of three representative filter samples of light (A), medium (B), and dark (C) BrC. (c) Same data as in (a) but also showing an exponential decay fit to the data (w = 7.6(\pm 0.4) $e^{-12.4(\pm 1.5)k_{550}}$; R-square = 0.9522) and the range of k550 (w = 0) of BC reported in Bond and Bergstrom. The BC values fall on the exponential decay function fitting the BrC data, indicating that BrC and BC fall on the same optical continuum.

The association between BrC darkness and volatility is illustrated in Figure 2 which shows mass fraction remaining (MFR) of BrC upon heating in the thermodenuder. The thermograms become less steep with increasing k, indicating that the BrC becomes less volatile with increasing darkness.

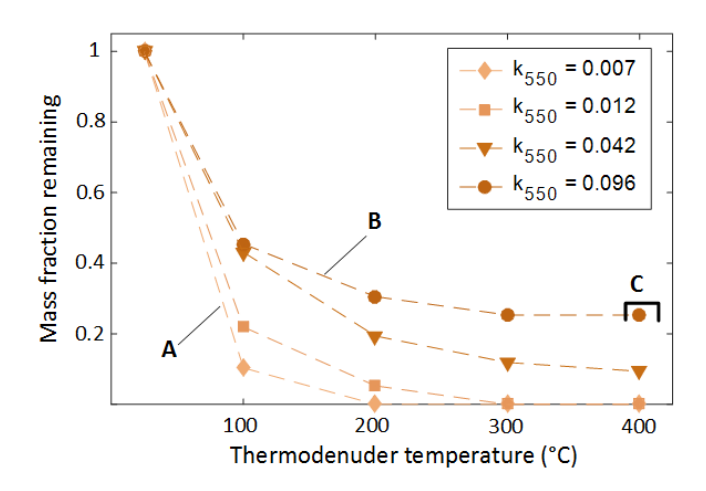
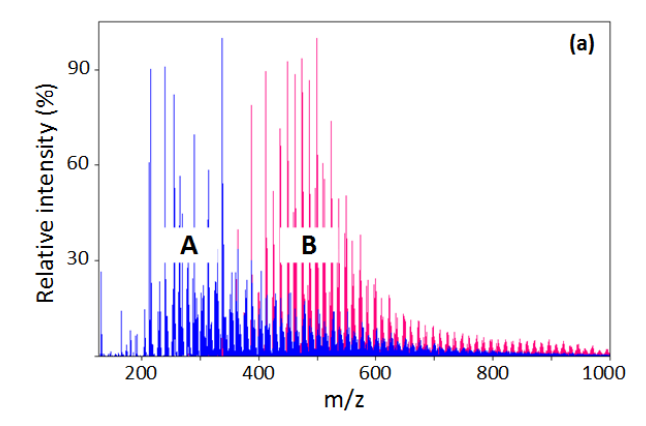


Figure 2 Thermograms showing mass fraction remaining (MFR) of benzene-combustion BrC with varying imaginary part of the refractive indices (k_{550}). Each data point represents a 30-minute average. The calculated standard deviations are smaller than the size of the symbols. The thermograms correspond to experiments 1, 2, 6, and 10 in Table S1. There is an inverse correlation between k_{550} (darkness) and the steepness of the thermograms (volatility). Thermograms **A** and **B** correspond to samples **A** and **B** in Figure 1, and **C** is the refractory BrC residual after heating to 400 °C.

To investigate the association between BrC darkness and molecular size, we performed LDI-MS analysis on the three samples A, B, and C. Figure 3a shows mass spectra of A and B up to m/z =1000. For both samples, we obtained regularly repetitive peaks separated by 24 u increments similar to those previously observed for soot precursors and could be explained by molecular growth of PAHs via the hydrogen abstraction - acetylene addition (HACA) mechanism.44 B exhibits molecular distributions that are shifted to larger sizes compared to A, confirming that the darker BrC is comprised of larger molecules. The mass spectra in Figure 3a were obtained with the detector operated at relatively low sensitivity dictated by saturating the signal of the highest peak. At this sensitivity, C exhibits no peaks in the m/z < 1000 range. The reason is that C constitutes the fraction of **B** that did not evaporate in the thermodenuder at 400 °C, which is the darkest, largest-molecular-size, and least-volatile fraction. To detect BrC at larger m/z values, the lower end of the m/z space was truncated at m/z = 1000, which allowed for operating the detector at a higher sensitivity. As shown in Figure S1, while B has higher intensities than C at low m/z, the two mass spectra converge at larger m/z and both exhibit peaks up to m/z \approx 5000. This suggests that the larger BrC molecules evaporated less than the smaller ones in the thermodenuder, which is to be expected since volatility depends on molecular size.⁵⁸ A zoom-in between m/z = 3300 and 4000 is given in Figure 3b, showing overlapping peaks of **B** and **C**. As expected from its relatively low k (Figure 1a) and high volatility (Figure 2), A exhibits no peaks in this large-molecular-size range.

These findings provide evidence that the continuum of BrC light-absorption properties (from light to dark) is associated with increase in molecular size and decrease in volatility. They also provide fundamentally based confirmation for previous reports that linked highly absorptive BrC to large-molecular-size³² and low-volatility^{7,59} organics.



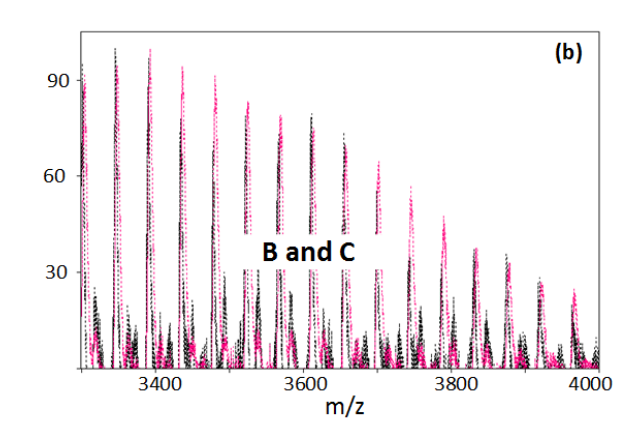


Figure 3 Mass spectra of three BrC samples (**A**, **B**, and **C**) emitted from benzene combustion with varying darkness (see Figure 1 for light-absorption properties) obtained using LDI-MS. (**a**) Mass spectra in the m/z < 1000 range of **A** and **B** obtained with a relatively low detector sensitivity dictated by saturating the signal of the highest peak. Sample **C** (the fraction of **B** that did not evaporate in the thermodenuder at 400 °C) shows no peaks in this m/z range. (**b**) Mass spectra of **B** (magenta) and **C** (black) in the 3300 – 4000 m/z range obtained by operating the detector at a higher sensitivity. The overlap between the two mass spectra in this large m/z range indicates that **C**, the low-volatility fraction of **B**, is comprised of the large-molecular-size fraction.

The darkest BrC we isolated corresponds to the residual after heating in the thermodenuder at $400 \,^{\circ}$ C, which we define as refractory BrC (rBrC). The k_{550} and w of rBrC in our experiments were 0.2-0.25 and 0.5-1, respectively, which are closer to BC ($k_{550} \approx 0.6$ -0.8 and $w \approx 0$) than the least-absorptive BrC we obtained in our experiments ($k_{550} = 0.004$ and w = 8.6). This indicates that the distinction between the light-absorption properties of BrC and BC is not as clear-cut as previously thought. rBrC is expected to be co-emitted with BC in real-life combustion and is likely to be lumped with BC (or elemental carbon – EC) in thermal-optical and incandescence measurements as well as light-absorption measurements which assume that only BC absorbs in the long-visible wavelengths.

We are confident that the data presented in this paper correspond to particles consisting solely of organic BrC molecules that did not contain BC. For the moderately absorbing particles, this follows directly from the complete evaporation in the thermodenuder (Figure 2), which confirms the absence of refractory material. For the highly absorbing particles, our assertion is based on size distribution measurements and scanning electron microscopy (SEM) imaging. As shown in Figure S2, the residual particles after heating in the thermodenuder at 400 °C were compact (near-spherical) and had a unimodal size distribution with a mode diameter smaller than 30 nm. On the other hand, BC formation was clearly identified by the formation of amorphous particles with mode diameters typically larger than 100 nm.

Since BrC has been mostly observed in biomass-combustion emissions, it is important to discuss the light-absorption properties we found in this study in the context of those reported for biomass-combustion BrC. Figure 4 presents a compilation of k_{550} values of biomass-combustion BrC obtained from various studies and grouped into three categories. The first category is BrC from low-temperature biomass combustion that produced only organics (no BC).^{3,4,56,57} This type of combustion is expected to produce a distribution of BrC products skewed towards the low-

absorbing side of the brown-black continuum, which is corroborated by the small k_{550} values. The second category is BrC from biomass combustion that also produced BC.6,7,27 k_{550} values of the second category are generally an order of magnitude larger than the first category. This is consistent with our brown-black continuum hypothesis because combustion that produces BC is expected to produce a distribution of BrC products skewed towards the highly absorbing side of the brown-black continuum. Isolating the low-volatility fraction of BrC constitutes the third category and yields further order-of-magnitude increase in k_{550} .7,26 This is also consistent with the brown-black continuum hypothesis because isolating the low-volatility fraction is essentially isolating the large-molecular-size BrC residing at the highly absorbing end of the continuum.

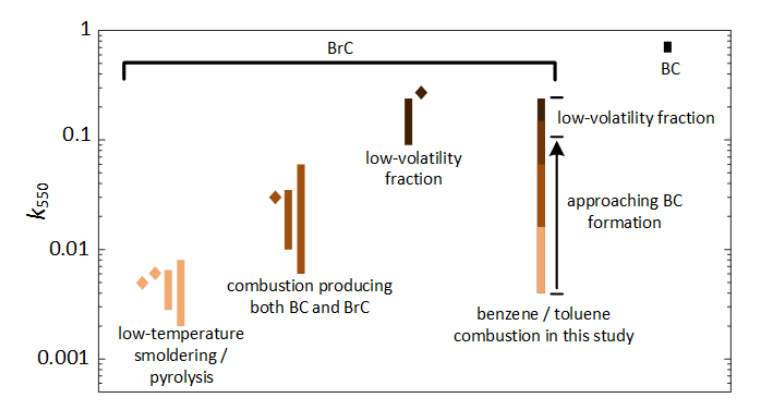


Figure 4 Ranges of the imaginary part of the refractive indices at 550 nm (k_550) of BrC in biomass-combustion emissions reported in the literature. Bars indicate ranges obtained from a certain study. The data are grouped in 3 categories: 1) BrC from low-temperature combustion (left to right: corn stalk pyrolysis, 57 wood pyrolysis, 3 peat smoldering 4,56); 2) BrC from biomass combustion that also produced BC (left to right: savanna fires, 27 combustion of boreal fuels, 6 combustion of boreal and grass fuels 7); 3) the low-volatility fraction of BrC. 7,26 Also shown is the range of k_{550} values obtained in this study from controlled benzene and toluene combustion, as well as k_{550} of BC. 20

Also shown in Figure 4 is the range of k_{550} obtained in this study and the range of BC k_{550} reported in Bond and Bergstrom.²⁰ By varying the combustion conditions, we could produce BrC with k_{550} that spanned those of smoldering and BC-producing biomass combustion. Furthermore, by isolating the low-volatility fraction via heating the BrC in the thermodenuder, we obtained k_{550} values similar to the low-volatility fraction of biomass-combustion emissions. This suggests that the BrC produced in real-life biomass combustion lies on the same brown-black continuum as the BrC produced in our experiments, thus supporting our assertion that a significant fraction of biomass-burning BrC is formed through the same pathways as BC.

Acknowledgments

We would like to thank Geoffrey Smith and his group for building the Multi-PAS III instrument for our group. The Multi-PAS III was essential to conducting this study. We would also like to thank the University of Georgia Proteomics and Mass Spectrometry Core Facility for performing LDI-MS analysis, Electron Microscopy facility for performing SEM imaging, and Scientific Glass Blowing Shop for construction of the combustion chamber used in this study. Financial support was provided by the National Science Foundation, Division of Atmospheric and Geospace Sciences (AGS- 1748080).

References

- (1) Andreae, M. O., and Gelencser, A. (2006) Black carbon or brown carbon? The nature of light-absorbing carbonaceous aerosols. *Atmos. Chem. Phys.* 6, 3131–3148.
- (2) Zhang, Y., Forrister, H., Liu, J., Dibb, J., Anderson, B., Schwarz, J. P., Perring, A. E., Jimenez, J. L., Campuzano-Jost, P., Wang, Y., Nenes, A., and Weber, R. J. (2017) Top-of-atmosphere radiative forcing affected by brown carbon in the upper troposphere. *Nat. Geosci.* 10, 486.
- (3) Chen, Y., and Bond, T. C. (2010) Light absorption by organic carbon from wood combustion. *Atmos. Chem. Phys.* 10, 1773–1787.
- (4) Chakrabarty, R. K., Moosmüller, H., Chen, L.-W. a., Lewis, K., Arnott, W. P., Mazzoleni, C., Dubey, M. K., Wold, C. E., Hao, W. M., and Kreidenweis, S. M. (2010) Brown carbon in tar balls from smoldering biomass combustion. *Atmos. Chem. Phys.* 10, 6363–6370.
- (5) Samburova, V., Connolly, J., Gyawali, M., Yatavelli, R. L. N., Watts, A. C., Chakrabarty, R. K., Zielinska, B., Moosmüller, H., and Khlystov, A. (2016) Polycyclic aromatic hydrocarbons in biomass-burning emissions and their contribution to light absorption and aerosol toxicity. *Sci. Total Environ.* 568, 391–401.
- (6) Saleh, R., Hennigan, C. J., McMeeking, G. R., Chuang, W. K., Robinson, E. S., Coe, H., Donahue, N. M., and Robinson, a. L. (2013) Absorptivity of brown carbon in fresh and photochemically aged biomass-burning emissions. *Atmos. Chem. Phys.* 13, 7683–7693.
- (7) Saleh, R., Robinson, E. S., Tkacik, D. S., Ahern, A. T., Liu, S., Aiken, A. C., Sullivan, R. C., Presto, A. A., Dubey, M. K., Yokelson, R. J., Donahue, N. M., and Robinson, A. L. (2014) Brownness of organics in aerosols from biomass burning linked to their black carbon content. *Nat. Geosci.* DOI: 10.1038/NGEO2220.
- (8) Pokhrel, R. P., Wagner, N. L., Langridge, J. M., Lack, D. a., Jayarathne, T., Stone, E. a., Stockwell, C. E., Yokelson, R. J., and Murphy, S. M. (2016) Parameterization of single-scattering albedo (SSA) and absorption Ångström exponent (AAE) with EC/OC for aerosol emissions from biomass burning. *Atmos. Chem. Phys.* 16, 9549–9561.
- (9) Lack, D. A., Langridge, J. M., Bahreini, R., Cappa, C. D., and Middlebrook, A. M. (2012) Brown carbon and internal mixing in biomass burning particles. *Proc. Natl. Acad. Sci. U. S. A.* 109, 14802–14807.
- (10) Lin, P., Bluvshtein, N., Rudich, Y., Nizkorodov, S. A., Laskin, J., and Laskin, A. (2017) Molecular Chemistry of Atmospheric Brown Carbon Inferred from a Nationwide Biomass Burning Event. *Environ. Sci. Technol.* 51, 11561–11570.
- (11) Lambe, A. T., Cappa, C. D., Massoli, P., Onasch, T. B., Forestieri, S. D., Martin, A. T., Cummings, M. J., Croasdale, D. R., Brune, W. H., Worsnop, D. R., and Davidovits, P. (2013) Relationship between oxidation level and optical properties of secondary organic aerosol. *Environ. Sci. Technol.* 47, 6349–57.
- (12) Updyke, K. M., Nguyen, T. B., and Nizkorodov, S. a. (2012) Formation of brown carbon via reactions of ammonia with secondary organic aerosols from biogenic and anthropogenic precursors. *Atmos. Environ.* 63, 22–31.
- (13) Zhong, M., and Jang, M. (2011) Light absorption coefficient measurement of SOA using a

- UV-Visible spectrometer connected with an integrating sphere. *Atmos. Environ.* 45, 4263–4271.
- (14) Liu, P. F., Abdelmalki, N., Hung, H.-M., Wang, Y., Brune, W. H., and Martin, S. T. (2015) Ultraviolet and visible complex refractive indices of secondary organic material produced by photooxidation of the aromatic compounds toluene and m-xylene. *Atmos. Chem. Phys.* 15, 1435–1446.
- (15) Moise, T., Flores, J. M., and Rudich, Y. (2015) Optical Properties of Secondary Organic Aerosols and Their Changes by Chemical Processes. *Chem. Rev.* 115, 4400–4439.
- (16) Jacobson, M. Z. (2000) A physically-based treatment of elemental carbon optics: Implications for global direct forcing of aerosols. *Geophys. Res. Lett.* 27, 217–220.
- (17) Jacobson, M. Z. (2001) Strong radiative heating due to the mixing state of black carbon in atmospheric aerosols. *Nature* 409, 695–7.
- (18) IPCC. (2014) Synthesis Report. Contribution of Working Groups I, II and III to the Fifth Assessment Report of the Intergovernmental Panel on Climate Change [Core Writing Team, R.K. Pachauri and L.A. Meyer (eds.)]. IPCC, Geneva, Switzerland,.
- (19) Bond, T. C., Doherty, S. J., Fahey, D. W., Forster, P. M., Berntsen, T., DeAngelo, B. J., Flanner, M. G., Ghan, S., Kärcher, B., Koch, D., Kinne, S., Kondo, Y., Quinn, P. K., Sarofim, M. C., Schultz, M. G., Schulz, M., Venkataraman, C., Zhang, H., Zhang, S., Bellouin, N., Guttikunda, S. K., Hopke, P. K., Jacobson, M. Z., Kaiser, J. W., Klimont, Z., Lohmann, U., Schwarz, J. P., Shindell, D., Storelvmo, T., Warren, S. G., and Zender, C. S. (2013) Bounding the role of black carbon in the climate system: A scientific assessment. *J. Geophys. Res. Atmos.* 118, 5380–5552.
- (20) Bond, T. C., and Bergstrom, R. W. (2005) Light Absorption by Carbonaceous Particles: An Investigative Review. *Aerosol Sci. Technol.* 39, 1–41.
- (21) Wang, X., Heald, C. L., Ridley, D. a., Schwarz, J. P., Spackman, J. R., Perring, a. E., Coe, H., Liu, D., and Clarke, a. D. (2014) Exploiting simultaneous observational constraints on mass and absorption to estimate the global direct radiative forcing of black carbon and brown carbon. *Atmos. Chem. Phys. Discuss.* 14, 17527–17583.
- (22) Saleh, R., Adams, P. J., Donahue, N. M., and Robinson, A. L. (2016) The interplay between assumed morphology and the direct radiative effect of light-absorbing organic aerosol. *Geophys. Res. Lett.* 43, 8735–8743.
- (23) Saleh, R., Marks, M., Heo, J., Adams, P. J., Donahue, N. M., and Robinson, A. L. (2015) Contribution of brown carbon and lensing to the direct radiative effect of carbonaceous aerosols from biomass and biofuel burning emissions. *J. Geophys. Res. Atmos*.
- (24) Zhou, C., Zhang, H., Zhao, S., and Li, J. On Effective Radiative Forcing of Partial Internally and Externally Mixed Aerosols and Their Effects on Global Climate. *J. Geophys. Res. Atmos.* 123, 401–423.
- (25) Laskin, A., Laskin, J., and Nizkorodov, S. a. (2015) Chemistry of Atmospheric Brown Carbon. *Chem. Rev.* DOI: 10.1021/cr5006167.
- (26) Alexander, D. T. L., Crozier, P. a, and Anderson, J. R. (2008) Brown carbon spheres in East Asian outflow and their optical properties. *Science* 321, 833–6.

- (27) Kirchstetter, T. W., Novakov, T., and Hobbs, P. V. (2004) Evidence that the spectral dependence of light absorption by aerosols is affected by organic carbon. *J. Geophys. Res.* 109, D21208.
- (28) Feng, Y., Ramanathan, V., and Kotamarthi, V. R. (2013) Brown carbon: a significant atmospheric absorber of solar radiation? *Atmos. Chem. Phys.* 13, 8607–8621.
- (29) Kordos, J. K., Scott, C. E., Farina, S. C., Lee, Y. H., L'Orange, C., Volckens, J., and Pierce, J. R. (2015) Uncertainties in global aerosols and climate effects due to biofuel emissions. *Atmos. Chem. Phys.* 15, 8577–8596.
- (30) Wang, Q., Saturno, J., Chi, X., Walter, D., Lavric, J. V., Moran-Zuloaga, D., Ditas, F., Pöhlker, C., Brito, J., Carbone, S., Artaxo, P., and Andreae, M. O. (2016) Modeling investigation of light absorbing aerosols in the central Amazon during the wet season. *Atmos. Chem. Phys.* 16, 14775–14794.
- (31) Liu, S., Aiken, A. C., Gorkowski, K., Dubey, M. K., Cappa, C. D., Williams, L. R., Herndon, S. C., Massoli, P., Fortner, E. C., Chhabra, P. S., Brooks, W. a., Onasch, T. B., Jayne, J. T., Worsnop, D. R., China, S., Sharma, N., Mazzoleni, C., Xu, L., Ng, N. L., Liu, D., Allan, J. D., Lee, J. D., Fleming, Z. L., Mohr, C., Zotter, P., Szidat, S., and Prévôt, A. S. H. (2015) Enhanced light absorption by mixed source black and brown carbon particles in UK winter. *Nat. Commun.* 6, 1–11.
- (32) Di Lorenzo, R. A., Washenfelder, R. A., Attwood, A. R., Guo, H., Xu, L., Ng, N. L., Weber, R. J., Baumann, K., Edgerton, E., and Young, C. J. (2017) Molecular-Size-Separated Brown Carbon Absorption for Biomass-Burning Aerosol at Multiple Field Sites. *Environ. Sci. Technol.* 51, 3128–3137.
- (33) Washenfelder, R. A., Attwood, A. R., Brock, C. A., Guo, H., L., X., Weber, R. J., Ng, N. L., Allen, H. M., Ayres, B. R., Baumann, K., Cohen, R. C., Draper, D. C., Duffey, K. C., Edgerton, E., Fry, J. L., Hu, W. ., Jimenez, J. L., Palm, B. B., Romer, P., Stone, E. A., Wooldridge, P. J., and Brown, S. S. Biomass burning dominates brown carbon absorption in the rural southeastern United States. *Geophys. Res. Lett.* 42, 653–664.
- (34) Lin, P., Aiona, P. K., Li, Y., Shiraiwa, M., Laskin, J., Nizkorodov, S. A., and Laskin, A. (2016) Molecular Characterization of Brown Carbon in Biomass Burning Aerosol Particles. *Environ. Sci. Technol.* 50, 11815–11824.
- (35) Claeys, M., Vermeylen, R., Yasmeen, F., Gómez-González, Y., Chi, X., Maenhaut, W., Mészáros, T., and Salma, I. (2012) Chemical characterisation of humic-like substances from urban, rural and tropical biomass burning environments using liquid chromatography with UV/vis photodiode array detection and electrospray ionisation mass spectrometry. *Environ. Chem.* 9, 273–284.
- (36) Yury, D., Yele, S., Xinhua, S., Taehyoung, L., Xinfeng, W., Tao, W., and L., C. J. Speciation of "brown" carbon in cloud water impacted by agricultural biomass burning in eastern China. *J. Geophys. Res. Atmos.* 118, 7389–7399.
- (37) Zhang, X. L., Lin, Y. H., Surratt, J. D., and Weber, R. J. (2013) Sources, Composition and Absorption Ångström Exponent of Light absorbing Organic Components in Aerosol Extracts from the Los Angeles Basin. *Environ. Sci. Technol.* 47, 3685–3693.

- (38) Phillips, S. M., and Smith, G. D. (2014) Light Absorption by Charge Transfer Complexes in Brown Carbon Aerosols. *Environ. Sci. Technol. Lett.* 382–386.
- (39) Hoffer, A., Tóth, Á., Pósfai, M., Chung, C. E., and Gelencsér, A. (2017) Brown carbon absorption in the red and near-infrared spectral region. *Atmos. Meas. Tech.* 10, 2353–2359.
- (40) Faccinetto, A., Desgroux, P., Ziskind, M., Therssen, E., and Focsa, C. (2011) High-sensitivity detection of polycyclic aromatic hydrocarbons adsorbed onto soot particles using laser desorption/laser ionization/time-of-flight mass spectrometry: An approach to studying the soot inception process in low-pressure flames. *Combust. Flame* 158, 227–239.
- (41) Desgroux, P., Mercier, X., and Thomson, K. a. (2013) Study of the formation of soot and its precursors in flames using optical diagnostics. *Proc. Combust. Inst.* 34, 1713–1738.
- (42) Solum, M. S., Sarofim, a. F., Pugmire, R. J., Fletcher, T. H., and Zhang, H. (2001) NMR analysis of soot produced from model compounds and a coal. *Energy and Fuels* 15, 961–971.
- (43) Stein, S. E., and Fahr, A. (1985) High-temperature stabilities of hydrocarbons. *J. Phys. Chem.* 89, 3714–3725.
- (44) Alfè, M., Apicella, B., Tregrossi, A., and Ciajolo, A. (2008) Identification of large polycyclic aromatic hydrocarbons in carbon particulates formed in a fuel-rich premixed ethylene flame. *Carbon N. Y.* 46, 2059–2066.
- (45) Apicella, B., Carpentieri, a., Alfè, M., Barbella, R., Tregrossi, a., Pucci, P., and Ciajolo, a. (2007) Mass spectrometric analysis of large PAH in a fuel-rich ethylene flame. *Proc. Combust. Inst.* 31 I, 547–553.
- (46) Apicella, B., Millan, M., Herod, a. a., Carpentieri, a., Pucci, P., and Ciajolo, a. (2006) Separation and measurement of flame-formed high molecular weight polycyclic aromatic hydrocarbons by size-exclusion chromatography and laser desorption/ionization time-of-flight mass spectrometry. *Rapid Commun. Mass Spectrom.* 20, 1104–1108.
- (47) Russo, C., Stanzione, F., Ciajolo, A., and Tregrossi, A. (2013) Study on the contribution of different molecular weight species to the absorption UV-Visible spectra of flame-formed carbon species. *Proc. Combust. Inst.* 34, 3661–3668.
- (48) Wang, H. (2011) Formation of nascent soot and other condensed-phase materials in flames. *Proc. Combust. Inst.* 33, 41–67.
- (49) Donahue, N. M., Epstein, S. A., Pandis, S. N., and Robinson, A. L. (2011) A two-dimensional volatility basis set: 1. organic-aerosol mixing thermodynamics. *Atmos. Chem. Phys.* 11, 3303–3318.
- (50) Qiao, L., Kim, C. H., and Faeth, G. M. (2005) Suppression effects of diluents on laminar premixed hydrogen/oxygen/ nitrogen flames. *Combust. Flame* 143, 79–96.
- (51) Chenglong, T., Zuohua, H., Jiajia, H., Chun, J., Xibin, W., and Haiyan, M. (2009) Effects of N2 dilution on laminar burning characteristics of propane-air premixed flames. *Energy and Fuels* 23, 151–156.
- (52) Fischer, A., and Smith, G. D. (2017) A Portable, Four-wavelength, Single-cell Photoacoustic Spectrometer for Ambient Aerosol Absorption. *Aerosol Sci. Technol.*
- (53) Faccinetto, A., Focsa, C., Desgroux, P., and Ziskind, M. (2015) Progress toward the

- Quantitative Analysis of PAHs Adsorbed on Soot by Laser Desorption/Laser Ionization/Time-of-Flight Mass Spectrometry. *Environ. Sci. Technol.* 49, 10510–10520.
- (54) Anna, C., Joachim, R. H., and Klaus, M. Clustering of polycyclic aromatic hydrocarbons in matrix-assisted laser desorption/ionization and laser desorption mass spectrometry. *Rapid Commun. Mass Spectrom.* 21, 2621–2628.
- (55) Apicella, B., Alfè, M., Amoresano, A., Galano, E., and Ciajolo, A. (2010) Advantages and limitations of laser desorption/ionization mass spectrometric techniques in the chemical characterization of complex carbonaceous materials. *Int. J. Mass Spectrom.* 295, 98–102.
- (56) Chakrabarty, R. K., Gyawali, M., Yatavelli, R. L. N., Pandey, A., Watts, A. C., Knue, J., Chen, L. W. A., Pattison, R. R., Tsibart, A., Samburova, V., and Moosmüller, H. (2016) Brown carbon aerosols from burning of boreal peatlands: Microphysical properties, emission factors, and implications for direct radiative forcing. *Atmos. Chem. Phys.* 16, 3033–3040.
- (57) Li, X., Chen, Y., and Bond, T. C. (2016) Light absorption of organic aerosol from pyrolysis of corn stalk. *Atmos. Environ.* 144, 249–256.
- (58) Donahue, N. M., Epstein, S. A., Pandis, S. N., and Robinson, A. L. (2011) A Two-Dimensional Volatility Basis Set: 1. Organic-Aerosol Mixing Thermodynamics.
- (59) Di Lorenzo, R. A., and Young, C. J. (2016) Size separation method for absorption characterization in brown carbon: Application to an aged biomass burning sample. *Geophys. Res. Lett.* 43, 458–465.